

Combination Fractional Carbon Dioxide Laser Treatment and Bone Marrow Mesenchymal Stem Cell Therapy Enhances the Treatment of Skin Photoaging in a Murine Model System

Li Li^{1-3,*}, Zeyu He^{1b 3-5,*}, Chengqian Yu³⁻⁵, Chao Zhang³⁻⁵, Yanqiu Yu⁶, Yuanhong Li³⁻⁵, Xuegang Xu³⁻⁵

¹ShanXi Medical University, Taiyuan, People's Republic of China; ²Department of Dermatology, The First Hospital of ShanXi Medical University, Taiyuan, 030001, People's Republic of China; ³Department of Dermatology, The First Hospital of China Medical University, Shenyang, 030001, People's Republic of China; ⁴Key Laboratory of Immunodermatology (China Medical University), Ministry of Education, Shenyang, 110001, People's Republic of China; ⁵NHC Key Laboratory of Immunodermatology (China Medical University), Shenyang, 110001, People's Republic of China; ⁶Department of Pathophysiology, College of Basic Medical Science, China Medical University, Shenyang, 110122, People's Republic of China

*These authors contributed equally to this work

Correspondence: Xuegang Xu, Department of Dermatology, The First Hospital of China Medical University, No. 155 Nanjing Bei Street, Heping District, Shenyang, Liaoning Province, 110001, People's Republic of China, Email xuxuegang2749290@163.com; Li Li, Department of Dermatology, The First Hospital of ShanXi Medical University, No. 85 South Jiefang Road, Yingze District, Taiyuan, Shanxi Province, 030001, People's Republic of China, Email lilizaimu0807@163.com

Background: Fractional carbon dioxide lasers and bone marrow mesenchymal stem cells (BMSCs) are commonly employed in the treatment of skin photoaging.

Objective: This study was developed to explore the effects of combination carbon dioxide laser treatment and BMSC injection on skin photoaging and the underlying molecular mechanisms.

Methods & Materials: In total, 24 mice with experimentally photoaged skin were separated into control, carbon dioxide fractional laser treatment, combination therapy, and BMSC injection groups. Samples of dorsal skin from these animals were subjected to hematoxylin and eosin staining or Masson's trichrome staining. In addition, immunohistochemical analyses and real-time polymerase chain reaction analyses were conducted to detect MMP-3 and MMP-9 expression.

Results: After 1 week, both dermal thickness and collagen fiber density were significantly increased in the BMSC and combination treatment groups as compared to the control group ($P < 0.05$), while both of these parameters were significantly increased in all treatment groups after 4 weeks relative to the control group ($P < 0.05$), with the most pronounced effect in the combination therapy group ($P < 0.05$). MMP-3 and MMP-9 mRNA and protein levels in the treatment groups were decreased relative to the control group after 4 weeks.

Conclusion: Combination BMSC and carbon dioxide laser therapy was more effective than either of these therapeutic approaches in isolation as a treatment for photoaged skin. The improvement of effect may be due to the decrease of MMP-3 and MMP-9 expression in combination therapy.

Keywords: bone marrow mesenchymal stem cell, fractional carbon dioxide laser, photoaging, matrix metalloproteinase, mouse model

Introduction

Cutaneous photoaging is the subject of growing research interest in light of the progressive increase in the average age of the global population. Indeed, given that maintaining a youthful appearance is often considered highly desirable, the global anti-aging products market was valued at \$191.7 billion in 2019. Cosmetics, injection therapies, and laser-based



treatments are now widely available to the public in an effort to combat photoaging, both novel evidence-based approaches are essential to improving the quality and range of extant treatment options.

Both chronological aging and extrinsic aging contribute to the aging of the skin, with extrinsic aging primarily being the result of cumulating damage resulting from ultraviolet (UV) radiation exposure, a process known as photoaging.¹ Photoaging is associated with clinical characteristics including the development of wrinkles, the thinning of the skin, desquamation, laxity, and telangiectasia.² Matrix metalloproteinase (MMP) activity has increasingly been identified as a key mediator of photoaging owing to the ability of these enzymes to degrade elastin and collagen within the skin.^{3,4}

Methods developed as treatments for photoaged skin to date include topical retinoid and antioxidant preparations as well as laser-based therapy. Owing to its ability to induce immediate collagen contraction followed by the delayed stimulation of collagen synthesis and remodeling, the use of an ultrapulse-mode CO₂ fractional laser represents a powerful approach to treating photoaged skin.^{5–7} Indeed, prior studies have conducted histological analyses confirming the efficacy of such treatment.⁸

Bone marrow mesenchymal stem cells (BMSCs) are stromal progenitor cells capable of undergoing rapid expansion, self-renewal, and differentiation into a range of tissue types.⁹ Recent research has shown that BMSCs play an important role as promoters of cutaneous healing owing to their ability to give rise to a range of skin cell types including keratinocytes and fibroblasts,¹⁰ contributing to *in vitro* and *in vivo* dermal tissue reconstruction.^{11,12}

Photoaging is still a burgeoning area of research, with an ever-evolving landscape of novel technologies and therapeutic strategies. Among the emerging frontiers in this field are the clinical applications and underlying mechanisms of stem cell therapies, which have become a focal point of intense interest. Our aim is to synergize the well-established CO₂ fractional laser technology with the intradermal administration of BMSC.

Here, we explored the efficacy of BMSC injection, ultrapulse-mode CO₂ fractional laser treatment, and a combination of these two treatments using a murine model of cutaneous photoaging. In addition, we conducted real-time polymerase chain reaction (RT-PCR) analyses and immunohistochemical staining aimed at confirming the molecular mechanisms underlying the observed efficacy.

Materials and Methods

BMSC Isolation, Culture, and Identification

Female C57BL/6 mice (4–6 weeks old; the Laboratory Animal Service Center of China Medical University, China) were euthanized, and BMSCs were harvested from the femurs of these animals. Following isolation, BMSCs were cultured in complete DMEM supplemented with 10% fetal bovine serum (FBS), 2 mm L-glutamine, and penicillin/streptomycin at 37°C in a 5% humidified CO₂ incubator, with passaging being performed when cells were 80–90% confluent. Cells were passaged three times prior to downstream use.

The ability of BMSCs to differentiate into different lineages was assessed as in our prior reports.¹³ In addition, flow cytometry was used to assess BMSC marker expression. Briefly, cells from the third passage were harvested and suspended in PBS at 10⁶ cells/mL, followed by two additional washes with PBS. Cells were then fixed for 5 min with 80% methanol at room temperature, followed by treatment for 20 min with 0.1% PBS-Tween (PBST) for 20 min. Cells were then blocked for 30 min with 5% BSA in PBS with constant agitation, followed by an additional wash with PBS. Cells (10⁶) were then suspended in 100 µL of 1x Annexin-binding buffer and stained for 30 min with anti-CD44-APC, anti-CD90-FITC, and anti-CD105-PE while protected from light. Cells were then washed once with PBS, suspended in 500 µL of PBS in a single-cell suspension, and analyzed via flow cytometry. Negative isotype control staining was additionally performed.

Murine Skin Photoaging Model

The Animal Experimentation Ethics Committee of the China Medical University approved this study. Female C57BL/6 mice (6–8 weeks old, 13–18 g) in the telogen phase were obtained from the Laboratory Animal Service Center of China Medical University. Animals were treated in strict accordance with international ethical guidelines and the National Institutes of Health Guide for the Care and Use of Laboratory Animals.

In total, 30 mice were randomly assigned to either a control group (n=6) or a photoaging model group (n=24). The backs of mice in the photoaging group were then shaved and exposed to UV light (Waldmann UV801K, Villingen-Schwenningen, Germany) with a UV-A + UV-B filter. Mice were positioned 30 cm from the source and underwent daily exposure over an 8-week period. During the telogen phase, the shaved skin of C57BL/6 mice typically appears pink, while slight redness of the dorsal skin was observed at the end of treatment (Table 1).

Therapeutic Interventions

Photoaged model mice were randomly assigned into four groups (n=6/group). Control animals did not undergo any additional treatment. Mice in the laser group were treated via a one-pass scan of the dorsal skin using the DeepFX™ microscanner handpiece for the ultrapulse-mode CO₂ fractional laser (Lumenis One™, Lumenis, CA, USA) with the following treatment parameters: pulse energy, 10 mJ; density, 10%; pulse size, 9 mm × 9 mm; and repetition rate, 600 hz. Mice in the BMSC treatment group received a subcutaneous injection of BMSCs (1 × 10⁵/mL, 1 mL/mouse) in the dorsal skin. Mice in the combination treatment group underwent both BMSC injection and CO₂ laser treatment as above using the same parameters defined for the monotherapy groups.

Macroscopic Observations

Samples of dorsal skin tissue were assessed for their roughness, elasticity, and wrinkles by two dermatologists blinded to experimental details at 1 and 4 weeks post-treatment (Table 2).

Histopathology

Samples of dorsal skin were collected following irradiation for 4 weeks and treatment for 1 or 4 weeks. Collected samples were fixed with 10% formalin overnight, paraffin-embedded, and cut into 5 mm-thick sections that were stained with hematoxylin and eosin (H&E) to conduct histological analyses, while changes in collagen fibers were assessed following Masson's trichrome staining. The percentage density and optical density values for collagen and elastic fibers were measured with Image-Pro Plus 6.0 (Media Cybernetics, PA, USA).

Immunohistochemistry

Immunohistochemical staining was performed by deparaffinizing samples and rehydrating them using xylene and an ethanol gradient, after which antigen retrieval was performed. Sections were then rinsed with PBS, blocked for 20 min with 5% goat serum at room temperature, and incubated overnight with primary rabbit anti-MMP3 (1:200; Abcam, Cambridge, UK) or rabbit anti-MMP9 (1:200; Abcam, Cambridge, UK) at 4°C. Samples were then stained for 15 min

Table 1 Procedure of Ultraviolet Irradiation

Time(week)	UVA	UVB
1–2	0.5J/cm ²	0.25 J/cm ²
3–5	1.0 J/cm ²	0.5 J/cm ²
6–8	1.5 J/cm ²	1.0 J/cm ²

Table 2 Grading Scales of Mouse Skin Wrinkling

Grade	Description of Mouse Wrinkles
0	No coarse wrinkles.
2	A few fine striations covering back which appear and disappear with motion.
4	Several shallow coarse wrinkles across back which are permanent.
6	Numerous deep coarse wrinkles across back which are permanent.

with secondary biotinylated goat anti-rabbit IgG at 37°C, followed by incubation for 30 min in an HRP-avidin solution at 37°C. Immunohistochemical signal detection was then conducted using 3,3'-diaminobenzidine, after which hematoxylin was applied for counterstaining. Sections were then rinsed under running water, dehydrated using an ethanol gradient, treated to transparency with xylene, sealed using neutral gum, and imaged via microscopy. Numbers of stained cells per section were counted using Image-Pro Plus 6.0.

Real-Time PCR

A miRNeasy Mini Kit (Qiagen, Hilden, Germany) was used based on provided directions to extract RNA from dorsal skin samples, after which a GoScript™ Reverse Transcription System (Promega, WI, USA) was used for cDNA preparation. All RT-PCR analyses were conducted with primers specific for *GAPDH* (forward: 5'-GGGCTCTCTGCTCCTCCCTGT, reverse: 5'-CGGCCAAATCCGTTACACCG), *MMP3* (forward: 5'-CCCCTGATGTCCTCGTGGTA, reverse: 5'-GCACATTGGTGATGTCTCAGGTT), and *MMP9* (forward: 5'-AGTGGGACCATCATAACATCACAT, reverse: 5'-TCTCGCGCAAGTCTTCAG) using a 7900HT Fast Real-Time PCR system (Applied Biosystems, MA, USA) with the following thermocycler settings: 95°C for 2 min; 40 cycles of 95°C for 15s, 60°C for 60s. Threshold cycle values were used to report collected data.

Statistical Analysis

Data were analyzed via one-way ANOVAs and Dunnett's test using SPSS v20.0 (SPSS, IL, USA), with $P < 0.05$ as the threshold of significance.

Results

Bone Marrow Mesenchymal Stem Cells Characterization

Previous studies have reported on the morphological characteristics and osteogenic/adipogenic differentiation capabilities of BMSCs.¹³ Here, we conducted a flow cytometry-based analysis of BMSC marker gene expression, revealing high levels of CD44 (100%), CD90 (99.0%), and CD105 (98.6%) positivity consistent with the identity of these cells as BMSCs (Figure 1). These results thus confirmed the successful isolation of cells that were functionally and morphologically consistent with BMSCs that were thus suitable for use in our experimental model system.

Skin Photoaging Model Establishment

Following UV irradiation for 8 weeks, the skin of mice in our skin photoaging model group exhibited deep wrinkles, a loss of elasticity, desquamation, and pigmentation that were not evident for mice in the control group (Figure 2). The H&E staining of these skin samples revealed a marked increase in epidermal thickness in the UV-irradiated group relative to non-irradiated control mice (Figure 2). Masson's trichrome staining revealed that the skin of irradiated mice

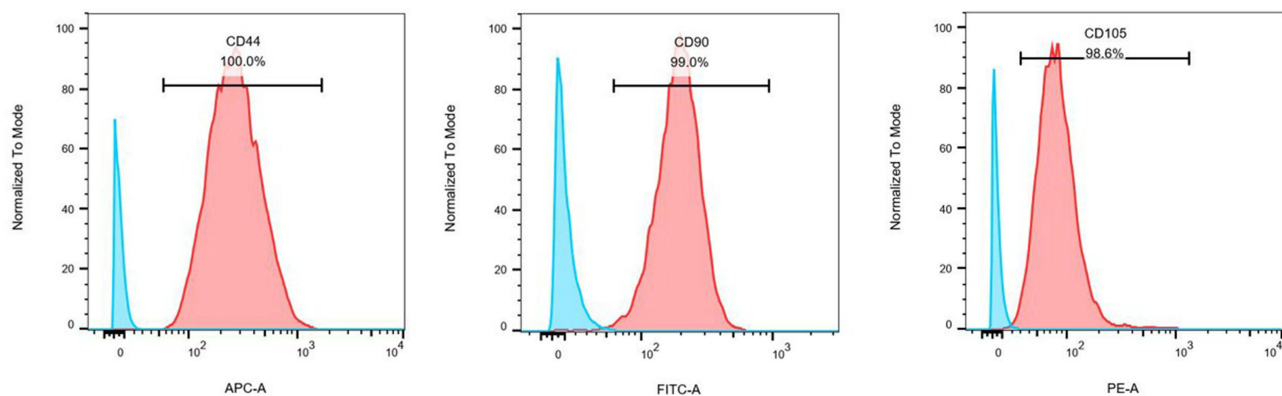


Figure 1 Flow cytometry analysis of bone marrow mesenchymal stem cells. BMSC surface antigen profiles were assessed via flow cytometry, revealing these cells to express the mesenchymal stem cell markers CD44, CD90, and CD105.

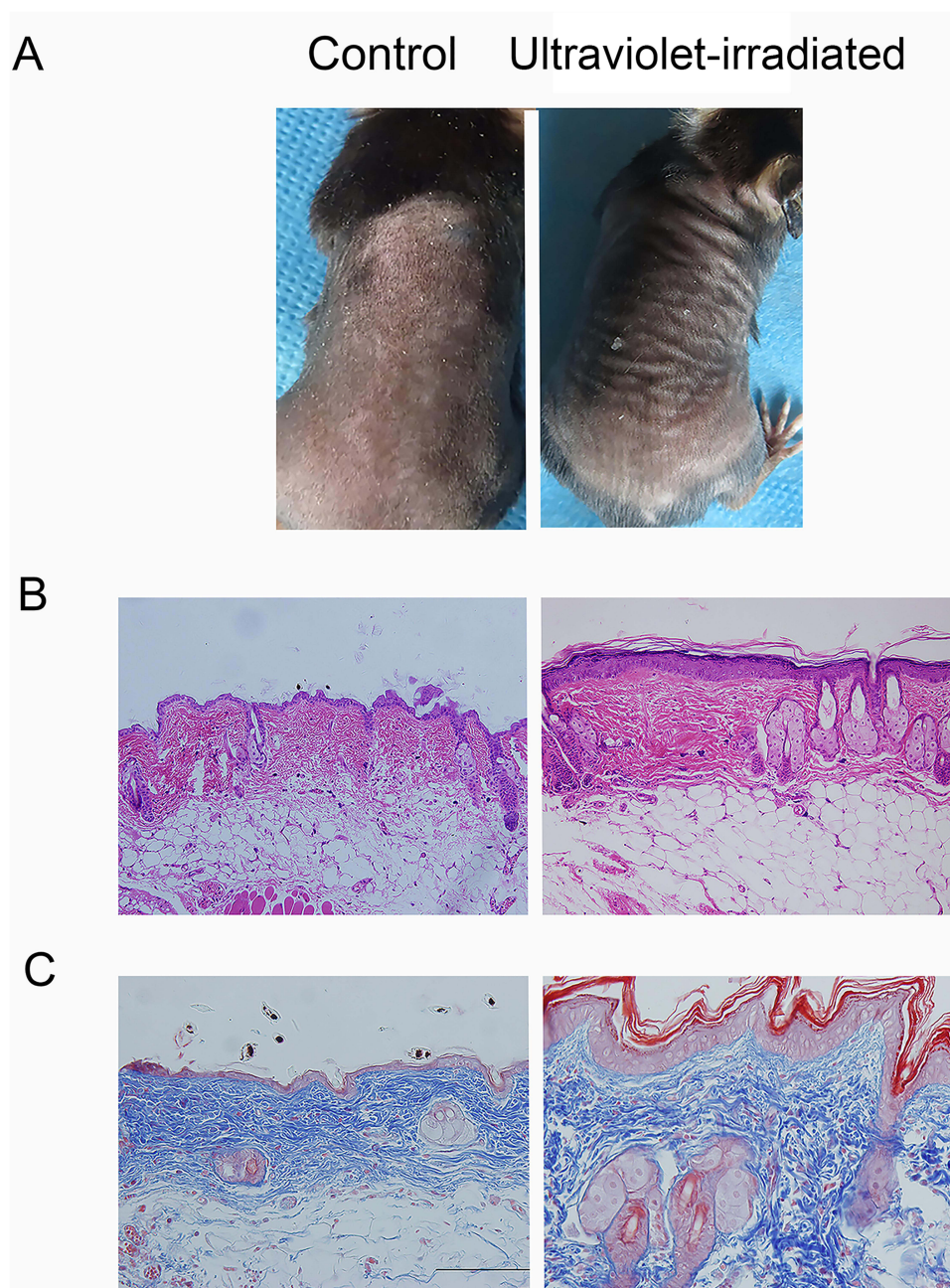


Figure 2 Murine skin photoaging model establishment. **(A)** Images of the skin surface for mice in the control (left) and UV-irradiated (right) groups after 8 weeks. **(B)** Hematoxylin and eosin staining of murine skin samples was conducted after 8 weeks (left: control; right: UV-irradiated group; 100 \times). **(C)** Masson's trichrome staining of murine skin samples was conducted after 8 weeks (left: control; right: UV-irradiated group; 100 \times).

also exhibited fewer collagen fibers, and those that were present were disordered relative to those observed in the skin of the non-irradiated mice (Figure 2).

Macroscopic Analyses of Treatment-Related Changes in Skin Photoaging Phenotypes

At 1-week post-treatment, fewer wrinkles and decreases skin roughness were evident in the BMSC and combination treatment groups relative to the photoaged control group, whereas no changes were observed in the laser treatment group. At 4-weeks post-treatment, there were significantly fewer wrinkles and smoother, more delicate skin in all three treatment groups as compared to the photoaged control group (Figure 3).

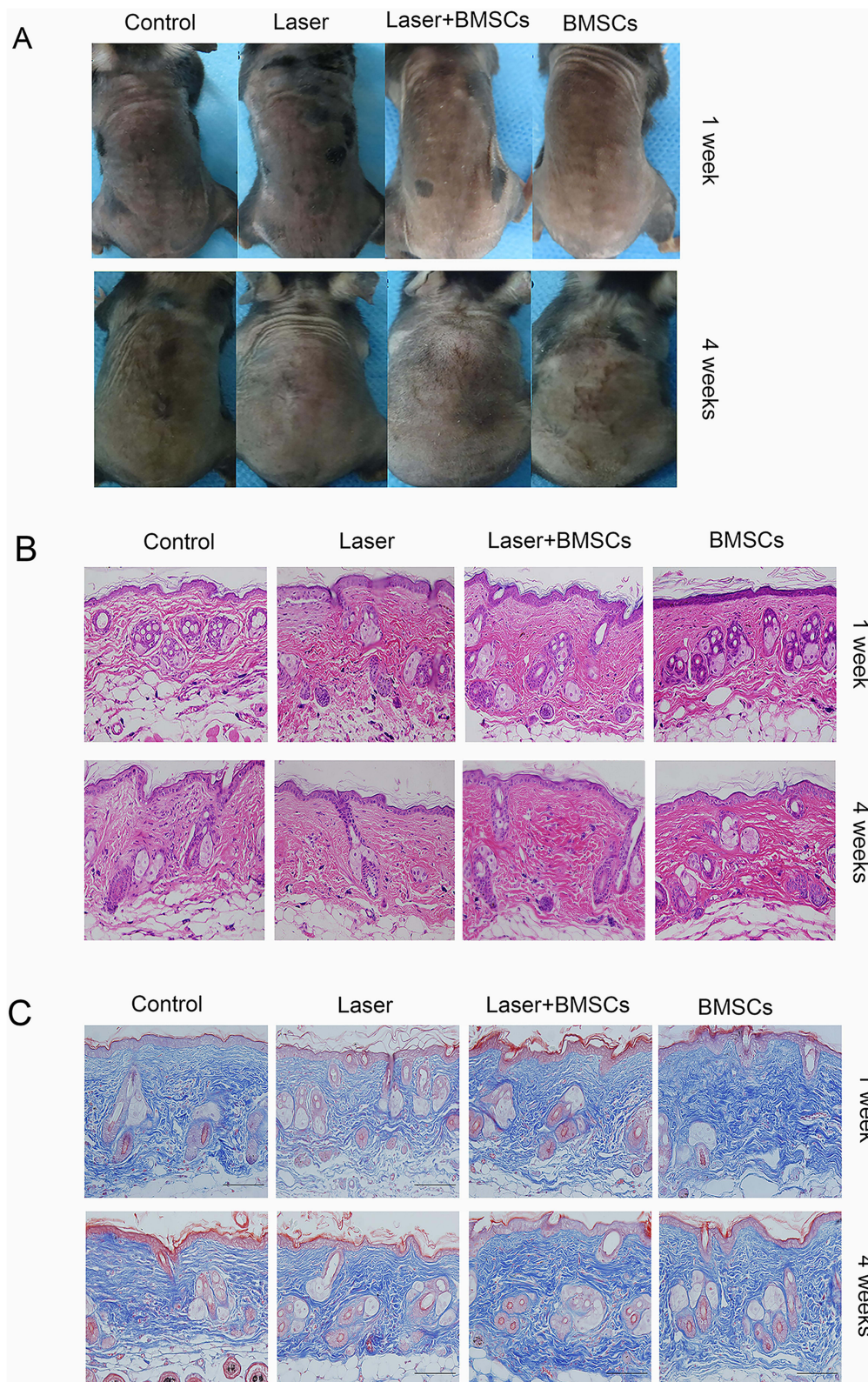


Figure 3 Clinical and histopathological analyses of photoaged murine following the application of different therapeutic regimens. **(A)** Images of the skin surface from mice in the control, laser, BMSC, and combination treatment groups following a 1- or 4-week post-treatment period. **(B)** Skin samples from the indicated groups were collected at 1 or 4 weeks post-treatment and subjected to hematoxylin and eosin staining (100 \times). **(C)** Skin samples from the indicated groups were collected at 1 or 4 weeks post-treatment and subjected to Masson's trichrome staining (400 \times).

At 1-week post-treatment, two dermatologists blinded to experimental grouping reported wrinkle scores that were significantly lower in the combination therapy (3.13 ± 0.43) and BMSC (3.42 ± 0.42) relative to photoaged controls (4.50 ± 0.43) ($P<0.05$), whereas differences in the laser group were not significant (3.88 ± 0.38) ($P>0.05$). At 4-weeks post-treatment, scores in all three treatment groups were significantly lower than that in the control group (3.17 ± 0.39) ($P<0.05$), with the combination group (1.50 ± 0.43) exhibiting a significantly lower score than that observed for both the laser group (2.58 ± 0.42) and the BMSC group (2.08 ± 0.29) ($P<0.05$), while there were no significant differences between these two +monotherapy groups ($P>0.05$)(Figure 4).

Histopathological Changes

At 1-week post-treatment, respective average dermal thickness values in the control, laser, combination, and BMSC treatment groups were $875.12\pm 166.25\ \mu\text{m}$, $952.57\pm 94.07\ \mu\text{m}$, $1116.60\pm 107.93\ \mu\text{m}$, and $1021.90\pm 113.96\ \mu\text{m}$. H&E staining revealed significant thickening of the dermal layer in the BMSC and combination treatment groups at this time point relative to the photoaged model group ($P<0.05$), with no significant difference between these two groups ($P>0.05$). As of 4-weeks post-treatment, the respective average dermal thickness values in the control, laser, combination, and BMSC treatment groups were $905.08\pm 178.16\ \mu\text{m}$, $1044.49\pm 161.73\ \mu\text{m}$, $1235.44\pm 158.39\ \mu\text{m}$, and $1099.13\pm 170.34\ \mu\text{m}$, with significant thickening of the dermis in all three treatment groups relative to the photoaged model control group, and with the dermal layer of mice in the combination therapy group being significantly increased relative to that of mice in any other treatment group ($P<0.05$; Figure 3)(Figure 4).

Masson's trichrome staining revealed significantly more dermal collagen fibers in each of the three treatment groups relative to the photoaged control group, with a significant increase in both percentage density and optical density values in the combination and BMSC treatment groups at 1-week post-treatment ($P<0.05$). Similarly, at 4-weeks post-treatment, all three treatment groups exhibited significant increases in collagen fiber density relative to the model control group, with these collagen fibers being arranged in a more regular manner following such treatment (Figure 3). Both the collagen percentage density and optical density values in each of these treatment groups were increased as compared to the control group, with significantly higher values in the combination group as compared to either monotherapy group ($P<0.05$) (Figure 5).

MMP-3 and MMP-9 Expression

Next, an immunohistochemical approach was used to evaluate MMP-3 and MMP-9 expression in skin samples from these animals, revealing that at the 1-week time point a reduction in MMP-9 expression was only evident in the BMSC groups, whereas at the 4-week time point both MMP-3 and MMP-9 levels were decreased in all three treatment groups as compared to the photoaged control group (Figure 6). RT-PCR further confirmed that at this 4-week time point, both MMP-3 and MMP-9 were downregulated in the treatment group relative to the control group ($P<0.05$), with no

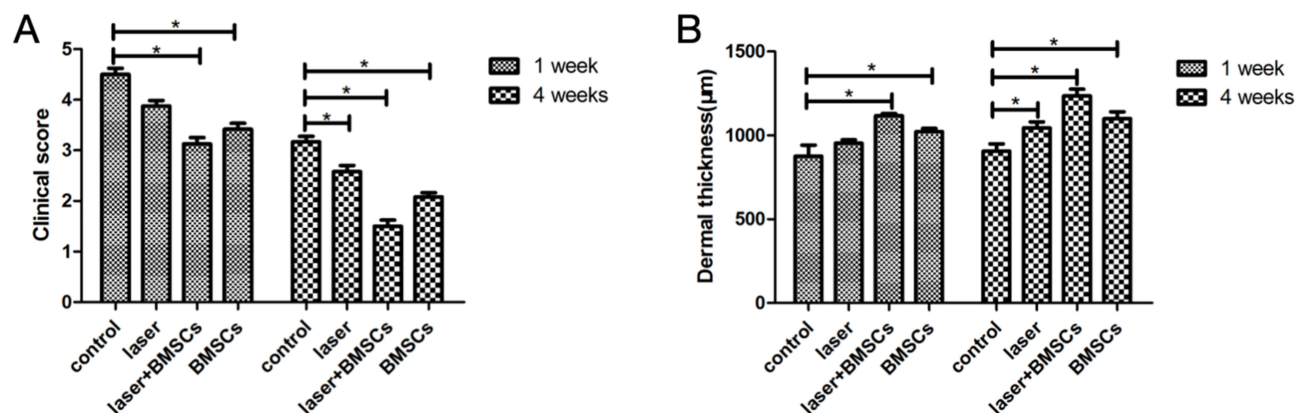


Figure 4 Assessment of clinical scores and skin thickness at 1 or 4 weeks post-treatment. (A) Clinical score of roughness, elasticity, and wrinkles. (B) Dermal thickness quantified from H&E staining. * $P<0.05$.

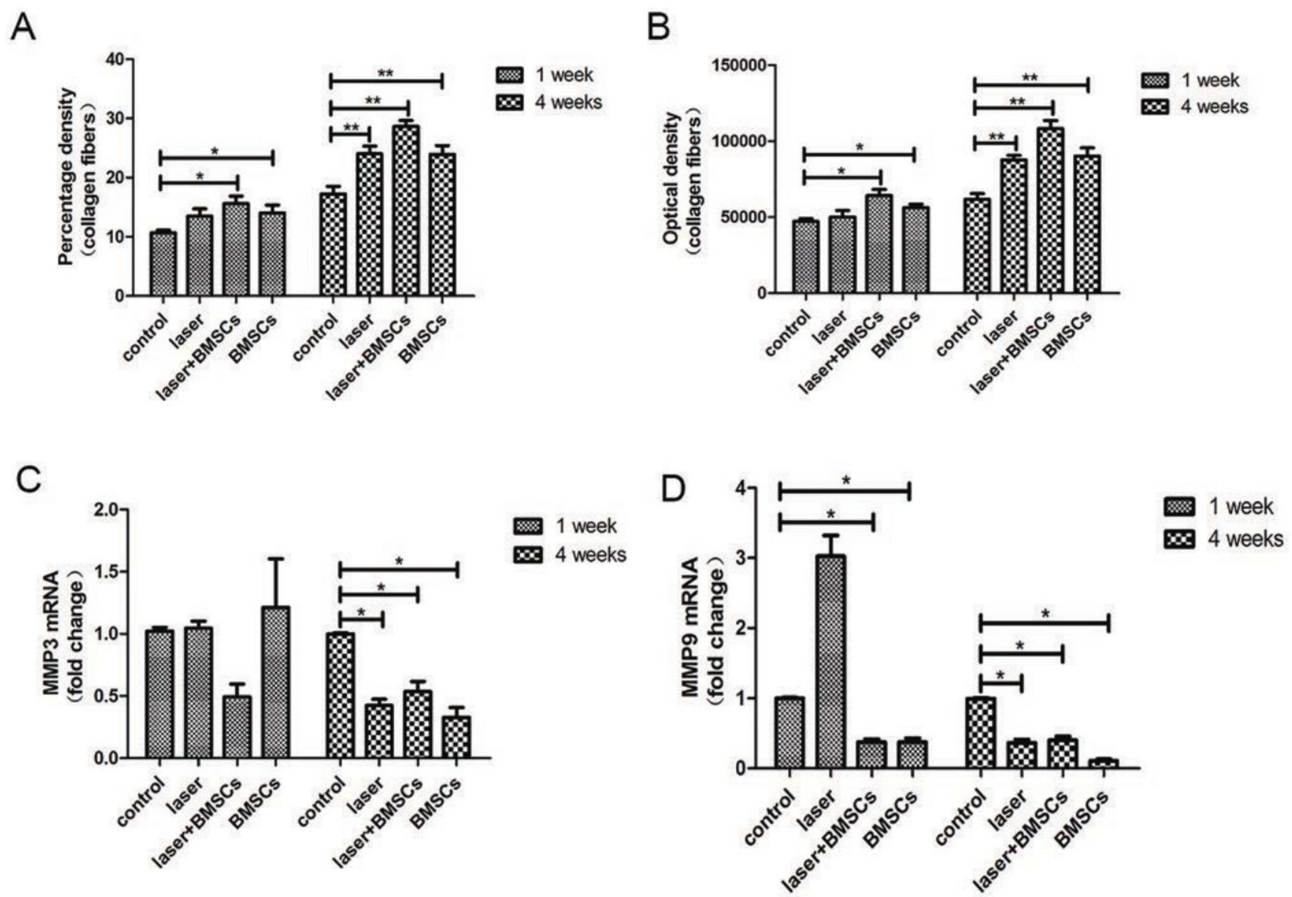


Figure 5 Assessment of collagen fibers and MMP-3/MMP-9 expression at 1 or 4 weeks post-treatment. **(A)** Collagen fiber density percentages. **(B)** Collagen fiber optical density. The mRNA levels of MMP-3 **(C)** and MMP-9 **(D)** were assessed at 1 week and 4 weeks post-treatment. * $P < 0.05$, ** $P < 0.01$.

significant differences among treatment groups ($P > 0.05$) (Figure 5). Moreover, at 1-week post-treatment, MMP-9 expression was significantly reduced in the BMSC and combination treatment groups as compared to the control group ($P < 0.05$), while MMP-9 expression in the laser group was elevated relative to that observed in the control group at this time point (Figure 5).

Discussion

Here, we explored the ability of BMSC injection and CO₂ laser treatments to ameliorate skin photoaging both as monotherapies and in combination with one another, and we explored the underlying mechanism of action. Through these analyses, we found that dermal thickening, increased collagen fiber density, and reduced MMP-3/MMP-9 expression were evident in the treatment groups relative to the photoaged control group at 4 weeks post-treatment.

Ever since hairless model mice were used by Sams et al to study UV irradiation-induced skin damage,¹⁴ these hairless animals have been widely employed in studies of cutaneous photoaging. In an effort to utilize a more cost-effective experimental system, we herein utilized C57BL/6 mice as experimental subjects and were able to successfully establish a model of skin photoaging. We did so by selecting C57BL/6 mice (6–8 weeks old) in the telogen hair follicle cycle phase, as characterized by a pink appearance to shaved skin. Consistent with the symptoms associated with chronic UV radiation exposure in clinical settings, our histological analyses revealed increased wrinkle formation and reduced collagen fiber density in these photoaged model mice, confirming the establishment of an appropriate model of skin photoaging.

Early studies seeking to utilize BMSCs for therapeutic purposes focused on experimentally differentiating these cells into specific cell types of interest, resulting in reported improvements in tissue function following transplantation that

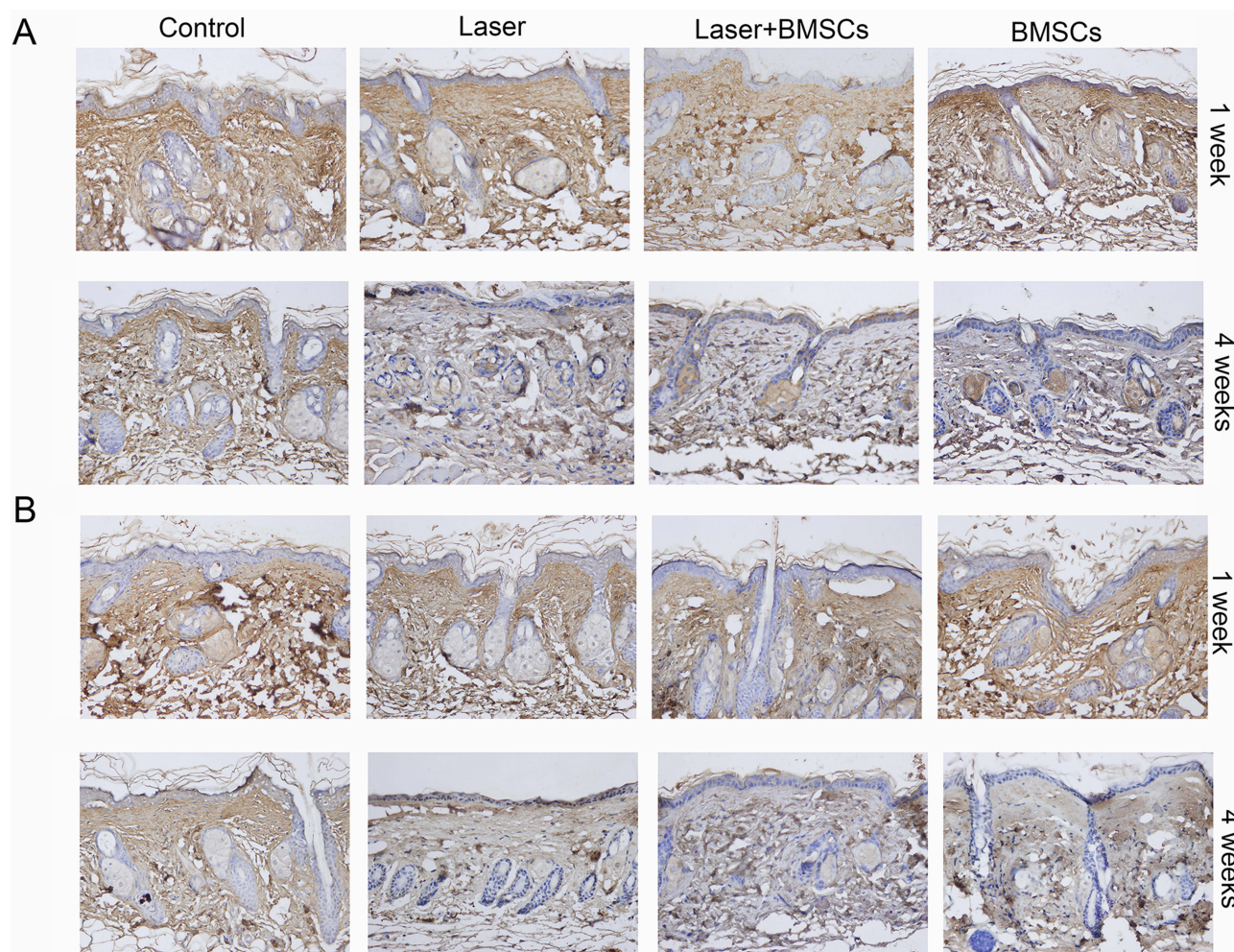


Figure 6 MMP-3 and MMP-9 in photoaged mouse skin. **(A)** MMP-3 expression at 1 week or 4 weeks post-treatment as measured via immunohistochemical staining (400 \times). Skin samples were collected from mice in the control, laser, BMSC, and combination treatment groups. **(B)** MMP-9 expression at 1 week or 4 weeks post-treatment as measured via immunohistochemical staining (400 \times).

were attributable to such differentiation. More recent research, however, has revealed that many of the functional benefits of stem cells may be attributable to their paracrine activity within host tissues rather than their ability to differentiate and repopulate recipient tissue niches.¹⁵ Several research groups have reported that BMSC transplantation is associated with significant improvements in photoaging, psoriasis, wound healing, hypertrophic scarring, and epidermolysis bullosa phenotypes.^{16,17} Increases in the activity of MMP family enzymes are closely tied to the pathogenesis of cutaneous photoaging, with increased MMP levels accelerating the breakdown of components of the dermal extracellular matrix including collagen and elastin fibers.^{18–20} Kwon et al previously explored the impact of BMSC treatment on photoaging, proliferation, MMP-1 expression, and type I collagen production in human dermal fibroblasts following UV-B exposure,²¹ revealing that BMSCs were able to suppress UV irradiation-induced MMP-1 upregulation while augmenting collagen synthesis. In line with our results, they reported that BMSCs exhibited robust anti-wrinkle properties, making them promising therapeutic tools when seeking to treat UV-induced skin damage.

Fractional photothermolysis resurfacing was first reported as an approach to cutaneous rejuvenation in 2004, and is now commonly employed as a treatment for several photoaging-related phenotypes including laxity, textural changes, and pigmentation.²² As each point exposed to the therapeutic laser generated a column of ablated and coagulated tissue around which the remaining skin is healthy, fractional photothermolysis ultimately produces microscopic thermal zones within the dermis and induces the rapid healing of these wounded areas.⁸ Ultrapulse-mode CO₂ lasers deliver a “flat-top” pulse beam with a short pulse duration and high fluency. In their previous analysis, Orringer et al assessed molecular

changes occurring in the context of dermal remodeling within photoaged human skin following CO₂ laser resurfacing, and observed the production of both type I and type III procollagen. Moreover, at 1-week post-treatment, they found that MMP-1, MMP-3, MMP-9, and MMP-13 mRNA levels were upregulated at 1-week post-treatment before decreasing several weeks thereafter,²³ leading these researchers to postulate that MMP upregulation may be associated with the breakdown of photodamaged collagen in the skin of these patients. Herein we sought to conduct a more detailed analysis of the mechanisms whereby BMSCs and CO₂ lasers can suppress photoaging, leading to our analyses of MMP expression. At 1 week after CO₂ laser treatment, we found MMP9 expression to be temporarily increased, whereas such expression was reduced at 4 weeks post-treatment.

The UV irradiation of skin can result in the excessive production of reactive oxygen species within cells,²⁴ contributing to increased MMP production and the consequent degradation of the extracellular matrix, thus driving photoaging.²⁵ MMP-3 and MMP-9 are respective members of the stromelysin and gelatinase subfamilies, and can thus degrade collagen and other extracellular matrix components in the skin. Inhibiting the expression or activity of MMP-3/MMP-9 is thus a key facet of any effort to prevent or treat photoaging. Herein, we found that CO₂ laser treatment and BMSC injection resulted in decreased MMP-3 and MMP-9 expression at the mRNA and protein levels at 4 weeks post-treatment, with a concomitant increase in collagen fiber density at this time point.

However, we found that the trend of MMP expression in the laser group of this experiment was variable, and we tried to explain this variation. The release of cytokines induced by the inflammatory response after thermal injury caused by CO₂ fractional laser^{26,27} and the proliferation and activation of fibroblasts during the repair process^{26,28} promote the expression of MMP. At a later stage, probably with the healing process, MMP expression is gradually suppressed, a process that may be related to the inhibitory effect of nascent collagen and other extracellular matrix components, thus reducing the degradation of nascent collagen and extracellular matrix.^{27,28} Possibly involved in this change is the MAPK signaling pathway: this pathway plays a key role in cell proliferation and differentiation. Laser treatment activates the MAPK signaling pathway, promoting fibroblast proliferation and MMP expression. As healing progresses, the activity of the MAPK pathway may gradually decrease, thus reducing MMP expression.²⁸

We also tried to analyze by what mechanism BMSC could reduce the expression of MMP-3 and MMP-9, NF-κB signaling pathway: BMSC also has an inhibitory effect on the intracellular nuclear factor κB (NF-κB) pathway. NF-κB is a key transcription factor involved in inflammatory responses and regulates the expression of a variety of cytokines and enzymes, including MMP3 and MMP9.²⁹ Cytokines: BMSC are able to secrete anti-inflammatory factors, such as IL-10 and TGF-β, which help to attenuate the inflammatory response and thus indirectly reduce MMP expression.³⁰ It can also alter the levels of pro-inflammatory cytokines (eg, IL-1β, IL-6) to reduce the pro-inflammatory response and thus reduce MMP expression.³¹ Exosomes: exosomes released by BMSC contain a variety of biologically active molecules, including mi-RNAs and proteins, which can bind to target cells and thus regulate the gene expression and function of these cells and inhibit MMP synthesis.³² Remodeling of the extracellular matrix: the presence of BMSC can promote the repair and remodeling of the extracellular matrix and inhibit excessive MMP expression, thus reducing cellular damage and inflammatory responses.³³

In conclusion, BMSC reduces the expression of MMP3 and MMP9 through multiple mechanisms, including inhibition of inflammatory signaling pathways, regulation of cytokines, exosome binding, and alteration of the extracellular matrix microenvironment. The interaction of these mechanisms makes BMSC show good therapeutic potential in diseases related to inflammation and tissue repair. Therefore, by combining CO₂ laser with BMSC, we hope to utilize the advantages of stem cells to enhance the treatment of photoaging.

BMSC injection can synergize with CO₂ laser treatment or the use of extracellular vesicles or conditioned media derived from a range of stem cell sources to protect the skin against UV-B-induced photoaging, thereby promoting cutaneous regeneration and wound healing.^{34–36} Our data are consistent with these prior reports. However, there are certain limitations to this study. For one, our sample size was limited, and only a small subset of genes and pathways were assessed when exploring the mechanisms governing the reversal of skin photoaging. As such, additional in-depth large-scale studies will be necessary to validate and expand upon our findings.

Conclusion

In summary, we herein found that both CO₂ laser treatment and BMSC injection were sufficient to ameliorate signs of skin photoaging in our mouse model system through mechanisms tied to enhanced collagen fiber production and the inhibition of MMP-3 and MMP-9 expression. Combination CO₂ laser treatment and BMSC injection was superior to either of these monotherapies in isolation, and may thus represent a promising therapeutic option for future use in the amelioration of cutaneous photoaging.

Acknowledgments

We thank Prof. Chen Hongduo, Prof. Wan Yinsheng, Prof. Song Bing, and Prof. Marco Stoller for helping to review this manuscript, and Prof. Ma Gang, Prof. Li Yuanhong for BMSC culture and data collection.

Funding

This study was supported by the National Natural Science Funding of China (82173443) and 111 project by the Ministry of Science and Technology (D18011).

Disclosure

The authors report no conflicts of interest in this work.

References

1. Fisher G, Kang S, Varani J, et al. Mechanisms of photoaging and chronological skin aging. *Arch Dermatol*. 2002;138(11):1462–1470.
2. Poon F, Kang S, Chien A. Mechanisms and treatments of photoaging. *Photodermatol Photoimmunol Photomed*. 2015;31(2):65–74. doi:10.1111/phpp.12145
3. Schwarz T. Photoimmunosuppression. *Photodermatol Photoimmunol Photomed*. 2002;18(3):141–145. doi:10.1034/j.1600-0781.2002.180307.x
4. Sun Z, Park S, Hwang E, et al. Salivianolic acid B protects normal human dermal fibroblasts against ultraviolet B irradiation-induced photoaging through mitogen-activated protein kinase and activator protein-1 pathways. *Photochemistry and Photobiology*. 2015;91(4):879–886. doi:10.1111/php.12427
5. Fitzpatrick R, Goldman M, Sriprachya-Anunt S. Resurfacing of photodamaged skin on the neck with an UltraPulse((R)) carbon dioxide laser. *Lasers Surg Med*. 2001;28(2):145–149. doi:10.1002/lsm.1030
6. Hantash B, Bedi V, Kapadia B, et al. In vivo histological evaluation of a novel ablative fractional resurfacing device. *Lasers Surg Med*. 2007;39(2):96–107. doi:10.1002/lsm.20468
7. Kilmer S, Chotzen V, Silva S, McClaren M. Safe and effective carbon dioxide laser skin resurfacing of the neck. *Lasers Surg Med*. 2006;38(7):653–657. doi:10.1002/lsm.20399
8. Xu X, Luo Y, Wu Y, et al. Immunohistological evaluation of skin responses after treatment using a fractional ultrapulse carbon dioxide laser on back skin. *Dermatologic Surg*. 2011;37(8):1141–1149. doi:10.1111/j.1524-4725.2011.02062.x
9. Ayatollahi M, Soleimani M, Geramizadeh B, Imanieh M. Insulin-like growth factor 1 (IGF-I) improves hepatic differentiation of human bone marrow-derived mesenchymal stem cells. *Cell Biol Int*. 2011;35(11):1169–1176. doi:10.1042/CBI20110016
10. Cui B, Zhang C, Gan B, et al. Collagen-tussah silk fibroin hybrid scaffolds loaded with bone mesenchymal stem cells promote skin wound repair in rats. *Mater Sci Eng C Mater Biol Appl*. 2020;109:110611. doi:10.1016/j.msec.2019.110611
11. Markowicz M, Koellensperger E, Neuss S, Koenigschulte S, Bindler C, Pallua N. Human bone marrow mesenchymal stem cells seeded on modified collagen improved dermal regeneration in vivo. *Cell Transplant*. 2006;15:723–732. doi:10.3727/000000006783464408
12. Vojtassák J, Danisovic L, Kubes M, et al. Autologous biograft and mesenchymal stem cells in treatment of the diabetic foot. *Neuro Endocrinol Lett*. 2006;27 Suppl 2:134–137.
13. Zhang C, Li Y, Qin J, et al. TMT-based quantitative proteomic analysis reveals the effect of bone marrow derived mesenchymal stem cell on hair follicle regeneration. *Front Pharmacol*. 2021;12:658040. doi:10.3389/fphar.2021.658040
14. Sams W, Smith J, Burk P. The experimental production of elastosis with ultraviolet light. *J Invest Dermatol*. 1964;43:467–471.
15. Baraniak P, McDevitt T. Stem cell paracrine actions and tissue regeneration. *Regen Med*. 2010;5(1):121–143. doi:10.2217/rme.09.74
16. Kim K, Blasco-Morente G, Cuende N, Arias-Santiago S. Mesenchymal stromal cells: properties and role in management of cutaneous diseases. *J Eur Acad Dermatol Venereol*. 2017;31(3):414–423. doi:10.1111/jdv.13934
17. Yu Y. Application of stem cell technology in antiaging and aging-related diseases. *Adv Exp Med Biol*. 2018;1086:255–265.
18. Kim J, Lee C, Kim E, et al. Inhibition effect of Gynura procumbens extract on UV-B-induced matrix-metalloproteinase expression in human dermal fibroblasts. *J Ethnopharmacol*. 2011;137(1):427–433. doi:10.1016/j.jep.2011.04.072
19. Misawa E, Tanaka M, Saito M, et al. Protective effects of aloe sterols against UVB-induced photoaging in hairless mice. *Photodermatol Photoimmunol Photomed*. 2017;33(2):101–111. doi:10.1111/phpp.12286
20. Pittayapruet P, Meephanan J, Prapapan O, Komine M, Ohtsuki M. Role of matrix metalloproteinases in photoaging and photocarcinogenesis. *Int J Mol Sci*. 2016;17(6):868. doi:10.3390/ijms17060868
21. Kwon T, Oh C, Choi E, et al. Conditioned medium from human bone marrow-derived mesenchymal stem cells promotes skin moisturization and effacement of wrinkles in UVB-irradiated SKH-1 hairless mice. *Photodermatol Photoimmunol Photomed*. 2016;32(3):120–128. doi:10.1111/phpp.12224

22. Manstein D, Herron G, Sink R, Tanner H, Anderson R. Fractional photothermolysis: a new concept for cutaneous remodeling using microscopic patterns of thermal injury. *Lasers Surg Med.* 2004;34(5):426–438. doi:10.1002/lsm.20048
23. Orringer J, Kang S, Johnson T, et al. Connective tissue remodeling induced by carbon dioxide laser resurfacing of photodamaged human skin. *Arch Dermatol.* 2004;140(11):1326–1332. doi:10.1001/archderm.140.11.1326
24. Chiang H, Chen H, Chiu H, Chen C, Wang S, Wen K. Neonauclea reticulata (Havil.) merr stimulates skin regeneration after UVB exposure via ROS scavenging and modulation of the MAPK/MMPs/Collagen pathway. *Evid Based Complement Alternat Med.* 2013;2013:324864. doi:10.1155/2013/324864
25. Liu S, You L, Zhao Y, Chang X. Hawthorn polyphenol extract inhibits UVB-induced skin photoaging by regulating MMP expression and type I procollagen production in mice. *J Agric Food Chem.* 2018;66(32):8537–8546. doi:10.1021/acs.jafc.8b02785
26. Shin JW, Kwon SH, Choi JY, et al. Molecular mechanisms of dermal aging and antiaging approaches. *Int J mol Sci.* 2019;20(9):2126. doi:10.3390/ijms20092126
27. Garza LA, Sheu M, Kim N, et al. Association of early clinical response to laser rejuvenation of photoaged skin with increased lipid metabolism and restoration of skin barrier function. *J Invest Dermatol.* 2023;143(3):374–385.e7. doi:10.1016/j.jid.2022.07.024
28. Reilly MJ, Cohen M, Hokugo A, Keller GS. Molecular effects of fractional carbon dioxide laser resurfacing on photodamaged human skin. *Arch Facial Plast Surg.* 2010;12(5):321–325. doi:10.1001/archfaci.2010.38
29. Fisher L. Expression of concern: bone marrow mesenchymal stem cells inhibited bleomycin-induced lung fibrosis. *RSC Adv.* 2022;12(8):4779. doi:10.1039/D2RA90008D
30. Ming J, Liao Y, Song W, et al. Role of intracranial bone marrow mesenchymal stem cells in stroke recovery: a focus on post-stroke inflammation and mitochondrial transfer. *Brain Res.* 2024;1837:148964. doi:10.1016/j.brainres.2024.148964
31. Gao L, Song Z, Mi J, et al. The effects and underlying mechanisms of cell therapy on blood-brain barrier integrity after ischemic stroke. *Curr Neuropharmacol.* 2020;18(12):1213–1226. doi:10.2174/1570159X18666200914162013
32. Cai H, Guo H. Mesenchymal stem cells and their exocytotic vesicles. *Int J mol Sci.* 2023;24(3):2085. doi:10.3390/ijms24032085
33. Satin AM, Norelli JB, Sgaglione NA, Grande DA. Effect of combined leukocyte-poor platelet-rich plasma and hyaluronic acid on bone marrow-derived mesenchymal stem cell and chondrocyte metabolism. *Cartilage.* 2021;13(2_suppl):267S–276S. doi:10.1177/1947603519858739
34. Xu X, Wang H, Zhang Y, et al. Adipose-derived stem cells cooperate with fractional carbon dioxide laser in antagonizing photoaging: a potential role of Wnt and β -catenin signaling. *Cell Biosci.* 2014;4:24. doi:10.1186/2045-3701-4-24
35. Xu P, Xin Y, Zhang Z, et al. Extracellular vesicles from adipose-derived stem cells ameliorate ultraviolet B-induced skin photoaging by attenuating reactive oxygen species production and inflammation. *Stem Cell Res Ther.* 2020;11(1):264. doi:10.1186/s13287-020-01777-6
36. Zhou B, Zhang T, Bin Jameel A, et al. The efficacy of conditioned media of adipose-derived stem cells combined with ablative carbon dioxide fractional resurfacing for atrophic acne scars and skin rejuvenation. *J Cosmet Laser Ther.* 2016;18(3):138–148. doi:10.3109/14764172.2015.1114638

Clinical, Cosmetic and Investigational Dermatology

Publish your work in this journal

Clinical, Cosmetic and Investigational Dermatology is an international, peer-reviewed, open access, online journal that focuses on the latest clinical and experimental research in all aspects of skin disease and cosmetic interventions. This journal is indexed on CAS. The manuscript management system is completely online and includes a very quick and fair peer-review system, which is all easy to use. Visit <http://www.dovepress.com/testimonials.php> to read real quotes from published authors.

Submit your manuscript here: <https://www.dovepress.com/clinical-cosmetic-and-investigational-dermatology-journal>

Dovepress
Taylor & Francis Group